

Optically induced anormal terahertz absorption in black silicon

Dong-Wei Zhai(翟东为), Hai-Ling Liu(刘海玲), Xxx Sedao, Yu-Ping Yang(杨玉平)
Citation: Chin. Phys. B . 2018, 27(2): 027802. **doi:** 10.1088/1674-1056/27/2/027802

Journal homepage: http://cpb.iphy.ac.cn; http://iopscience.iop.org/cpb

What follows is a list of articles you may be interested in

Closed-form internal impedance model and characterization of mixed carbon nanotube bundles for three-dimensional integrated circuits

Qijun Lu(卢启军), Zhangming Zhu(朱樟明), Yintang Yang(杨银堂), Ruixue Ding(丁瑞雪), Yuejin Li(李跃进)
Chin. Phys. B . 2018, 27(1): 017303. **doi:** 10.1088/1674-1056/27/1/017303

Dynamic localization of two electrons in AC-driven triple quantum dots and quantum dot shuttles

Jin-Xian Qu(屈晋先), Su-Qing Duan(段素青), Ning Yang(杨宁)
Chin. Phys. B . 2017, 26(12): 127308. **doi:** 10.1088/1674-1056/26/12/127308

Photon-assisted electronic and spin transport through two T-shaped three-quantum-dot molecules embedded in an Aharonov-Bohm interferometer

Jiyuan Bai(白继元), Li Li(李立), Zelong He(贺泽龙), Shujiang Ye(叶树江), Shujun Zhao(赵树军), Suihu Dang(党随虎), Weimin Sun(孙伟民)
Chin. Phys. B . 2017, 26(11): 117302. **doi:** 10.1088/1674-1056/26/11/117302

Polaron effects in cylindrical GaAs/$Al_xGa_{1-x}As$ core-shell nanowires

Hui Sun(孙慧), Bing-Can Liu(刘炳灿), Qiang Tian(田强)
Chin. Phys. B . 2017, 26(9): 097302. **doi:** 10.1088/1674-1056/26/9/097302

Terahertz time-domain spectroscopy of a simulated pore structure to probe particle size and porosity of porous rock

Dong Chen, Bao Ri-Ma, Zhao Kun, Xu Chang-Hong, Jin Wu-Jun, Zhong Shou-Xian
Chin. Phys. B . 2014, 23(12): 127802. **doi:** 10.1088/1674-1056/23/12/127802

Optically induced abnormal terahertz absorption in black silicon*

Dong-Wei Zhai(翟东为)[1], Hai-Ling Liu(刘海玲)[1], Xxx Sedao[2], and Yu-Ping Yang(杨玉平)[1,†]

[1] *School of Science, Minzu University of China, Beijing* 100081, *China*
[2] *Labo Hubert Curien, University of Lyon, France*

(Received 7 July 2017; revised manuscript received 8 October 2017; published online 5 January 2018)

The absorption responses of blank silicon and black silicon (silicon with micro/nano-conical surface structures) wafers to an 808-nm continuous-wave (CW) laser are investigated at room temperature by terahertz time-domain spectroscopy. The transmission of the blank silicon shows an appreciable change, from ground state to the pump state, with amplitude varying up to 50%, while that of the black silicon (BS) with different cone sizes is observed to be more stable. Furthermore, the terahertz transmission through BS is observed to be strongly dependent on the size of the conical structure geometry. The conductivities of blank silicon and BS are extracted from the experimental data with and without pumping. The non-photo-excited conductivities increase with increasing frequency and agree well with the Lorentz model, whereas the photo-excited conductivities decrease with increasing frequency and fit well with the Drude–Smith model. Indeed, for BS, the conductivity, electron density and mobility are found to correlate closely with the size of the conical structure. This is attributed to the influence of space confinement on the carrier excitation, that is, the carriers excited at the BS conical structure surface have a stronger localization effect with a backscattering behavior in small-sized microstructures and a higher recombination rate due to increased electron interaction and collision with electrons, interfaces and grain boundaries.

Keywords: terahertz spectroscopy, black silicon, ultrafast phenomena

PACS: 78.47.jh, 73.63.–b, 42.65.Re **DOI:** 10.1088/1674-1056/27/2/027802

1. Introduction

Black silicon (BS) is a term used to describe silicon with micro (and/or nano)-scale conical surface structures that are induced by short and ultrafast laser pulse irradiation or plasma etching.[1–3] Because of its strong absorption in the visible light and infrared regime, BS has drawn a great deal of attention for its optoelectronic applications like light harvesting in solar cells and light-emitting devices.[4,5] The BS formed in SF_6, featuring a narrowed band gap due to the sulfur doping, has a broad spectral band of absorption, extending to the THz.[6] For BS structured in air, without band gap modification the strong spectral absorption band ends at 1200 nm, making it potentially useful for enhancing the emission of THz radiation from natural surface emitter.[7] However, the absorption of the enhanced THz emission, changed by BS micro (nano)-structured surface, to the best of our knowledge, has not been comprehensively studied, which is probably because the identifying of localization effects and ultrafast carrier dynamics of micro- (or nano-) structured surface is not trivial, and they exhibit process-dependent and surface-sensitive properties.

Terahertz time-domain spectroscopy (THz-TDS) is an excellent technique for studying optical properties of various materials including semi-conductors and conducting polymers in forms of nanoparticles, nanowires, nanodisks, hollow spheres, etc.[8–13] It probes the far-infrared (30 μm–3 mm, 0.1 THz–10 THz) region of the spectrum, which closely matches typical carrier scattering rates of 10^{12} s^{-1} to 10^{14} s^{-1}.[14–16] Furthermore, THz transmission or absorption is sensitive to the density and transportation of carriers. Thus, THz-TDS can directly infer the influence of micro (nano)-scale disorder and size effect on carrier motion from the response of surface conical structure to electromagnetic field in the terahertz frequency range. In this study, we report the absorption responses of blank silicon and BS wafers to an 808-nm continuous-wave (CW) laser at room temperature by terahertz time-domain spectroscopy system (THz-TDS).

2. Experimental methods and results

The micro (or nano)-structured surface geometry used in the experiment was fabricated by direct-laser-writing (DLW) technique on a double-side polished ⟨100⟩ Si wafer with a resistivity of 1000 Ω·cm. Compared with the conventional fabrication methods such as plasma or chemical etching, DLW is simple and cost effective.[17–19] In addition, the DLW technique allows for precise control over the dimensions of the surface micro-structures and enables systematic and highly reproducible studies of its geometry-dependent optical properties. In air, the BS was micro-structured by a solid-state nano-second laser (Enpon-Nano-H532) with a 355-nm wave-

*Project supported by the National Natural Science Foundation of China (Grant Nos. 11574408, 11504439, 61627814, and 61675238), the National Key Research and Development Program of China (Grant No. 2017YFB0405402), the National Instrumentation Program of China (Grant No. 2012YQ14000508), and the Young-talent Plan of State Affairs Commission, China (Grant No. 2016-3-02).

†Corresponding author. E-mail: ypyang_cun@126.com

© 2018 Chinese Physical Society and IOP Publishing Ltd

length and 6-ns pulse duration. The wafers were ultrasonically cleaned in an acetone bath, and then dried in a nitrogen gas flow. The laser fluence was fixed at 11.8 J/cm^2. By controlling the laser scanning speed, overlap ratio and intervals between successive laser scan tracks, we obtained four microstructured BS surfaces (numbered 01, 02, 03 and 04, accordingly), with increasing unity size as shown in Fig. 1.

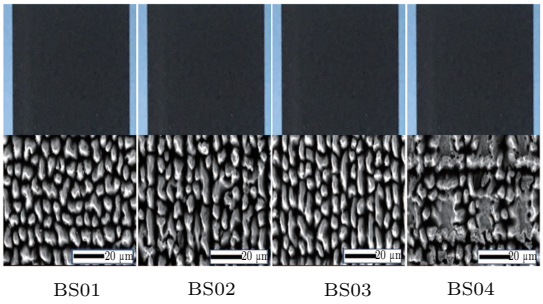


Fig. 1. (color online) Four BS samples and their scanning electron micrographs. The sizes of surface conical structure are approximately 5 μm–8 μm (BS01), 8 μm–15 μm (BS02), 18 μm–25 μm (BS03), 30 μm–40 μm (BS04), respectively.

We measured the total (specular and diffuse) reflectance (R) and transmittance (T) to determine the absorptance ($A = 1 - R - T$) of the structured surfaces in spectrum range from 620 nm to 1050 nm. The measurements were performed by using a spectrophotometer equipped with an integrating sphere detector. Figure 2 shows the wavelength-dependent absorptions of the structured BS surfaces and blank silicon. The absorption of the BS is evidently twice superior to that of the blank silicon over the spectrum range investigated. Thus, any wavelength in the range is suitable for the following THz experiment.

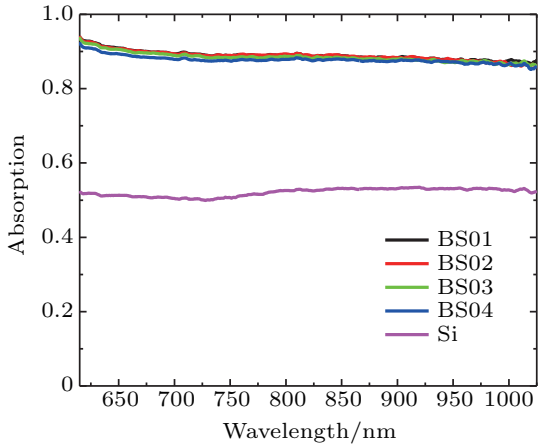


Fig. 2. (color online) Absorptions of four BS and Si wafers in the spectrum range from 620 nm to 1050 nm.

We characterized absorption tunabilities of blank silicon and BS by using a terahertz time-domain spectroscopy system with a couple of photoconductive antennas for both terahertz generation and detection as shown in Fig. 3. A mode-locked Ti: sapphire laser with a central wavelength of 800 nm, pulse duration of 100 fs, and repetition rate of 82 MHz was used as an optical source. An all-solid-state CW laser (808 nm, 4.8 W/cm^2) was used as an external pumping source to excite photo-generated carriers in the silicon wafers. The spot diameters of THz beam and the CW laser were about 8 mm and 15 mm, respectively. The detailed description of the system setup and data handling can be found in previous work.[20]

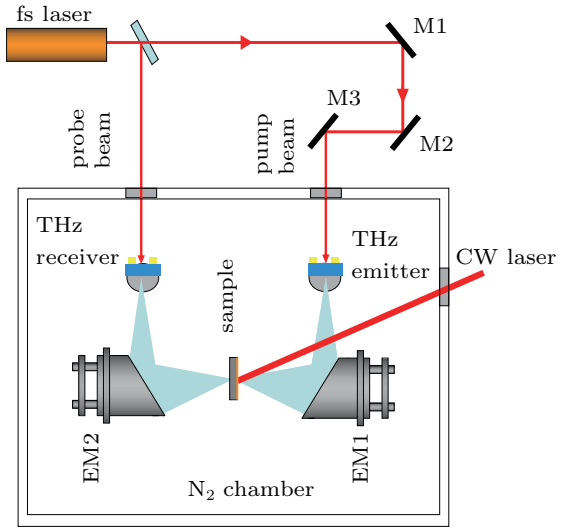


Fig. 3. (color online) THz-TDS system with optical modulation used for absorption tenability experiment.

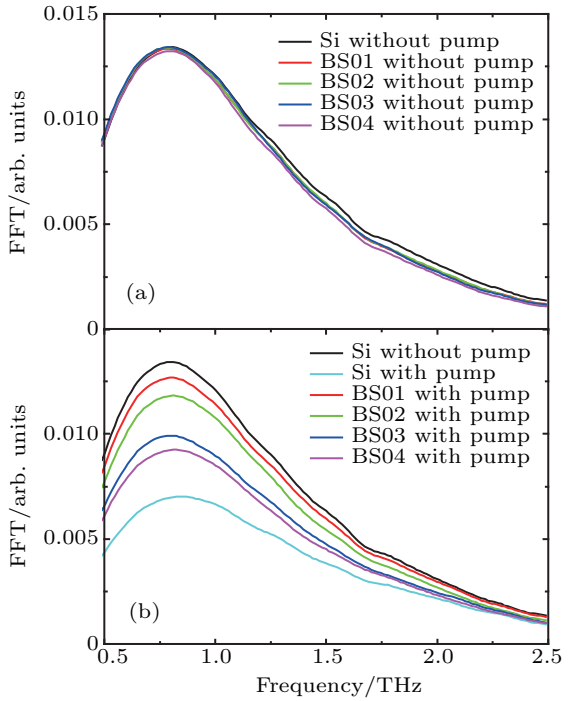


Fig. 4. (color online) Transmitted THz spectra of Si wafers with smooth and micro-structured (a) without pumping and (b) with 4.8-W/cm^2 optical pumping.

The transmitted THz spectra of two different structure types, i.e., blank silicon and BS, without and with optical pumping, are shown in Figs. 4(a) and 4(b). As can be seen in Fig. 4(a), without optical pumping, the spectra of the two structure types differ very little throughout 0.5 THz–2.5 THz spectrum range. It implies that without pumping, the THz

transmission is independent of surface micro-structure. However, under a 4.8-W/cm^2 optical pumping, the transmitted spectra (see in Fig. 4(b)) exhibit a pronounced difference between structured and unstructured silicon. The transmission of blank silicon with smooth surface strongly decreases and the residual transmission is less than 50%, whereas the transmission of the BS is much less influenced by optical pumping. In addition, four BS samples with different geometric structures show transmissions different from each other: the greater the surface micro-structure unity size, the lower the THz transmission is.

3. Discussion

The BS absorption at 808-nm pump beam is twice more than the blank silicon absorption. Furthermore, the THz-TDS experimental results show that, without pump, the THz transmission is independent of surface micro-structure. Thus, we attribute the abnormal THz absorption by BS under optical pumping to special carrier dynamics in surface micro-structure.

In order to explain the proposed mechanism of photo-generated carrier dynamics and validate our hypothesis, the real part of conductivity of the refractive index n of the sample through the relationship:

$$\sigma_{\mathrm{r}}(\omega) = \varepsilon_0 \alpha c n, \tag{1}$$

where ε_0 is the dielectric constant in vacuum and c is the velocity of light. The frequency dependence and n are extracted from the experimental data by using the well-known amplitude transmission function of a parallel dielectric slab:[21]

$$n(\omega) = \frac{\varphi(\omega) c}{\omega} + 1, \tag{2}$$

$$\alpha(\omega) = \frac{2}{d} \frac{4n(\omega)}{A(\omega)\left[n(\omega)+1\right]^2}, \tag{3}$$

where ω is the angular frequency of the incident THz wave, d is the thickness of the sample, $A(\omega)$ and $\varphi(\omega)$ are the frequency-dependent amplitude ratio and phase difference between the Fourier analysis of reference ($\tilde{E}_{\mathrm{refer}}$) and sample ($\tilde{E}_{\mathrm{sample}}$) pulse, respectively. The empty circles in Fig. 5 represent the real part of conductivity as a function of frequency varying from 0.5 THz to 1.5 THz without pumping. As can be seen, the native conductivity of sample is calculated for comparison and it is determined by the absorption coefficient and the samples increase with increasing frequency. For a perfect semiconductor crystal, optical response in the far-infrared (or THz) region is attributed to the lattice vibrations. According to the Lorentz dispersion theory, the real part of conductivity can be described as follows:[22]

$$\sigma_{\mathrm{r}} = \frac{(Ne^2/m^*)\gamma\omega^2}{\left(\omega_0^2 - \omega^2\right)^2 + \gamma^2\omega^2}, \tag{4}$$

where N is the electron density, e is the elementary charge, m^* is the electron effective mass, ω_0 and ω are the angular frequency, and γ is the damping constant. Using Eq. (4), the calculated conductivities for both blank and black silicon wafers (solid curves in Fig. 5) can achieve a good agreement with the experimental data above and the results in Fig. 4(a). In addition, we can calculate the average value of $\omega_0/2\pi$, which is 15.79 THz and close to the frequency of the transverse optical (TO) mode located at 525 cm^{-1}, which is equal to 15.75 THz.[23]

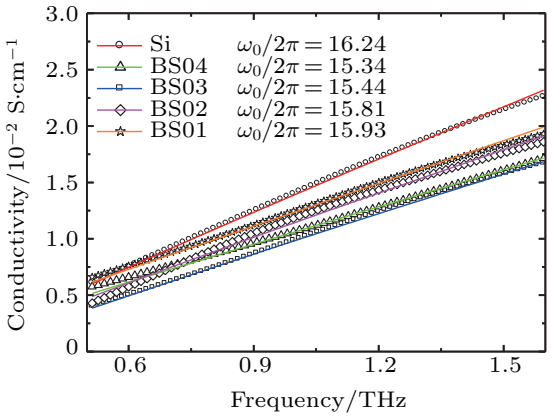


Fig. 5. (color online) Plots of non-photo-excited conductivities of Si, BS01, BS02, BS03, and BS04 without optical pump versus frequency, where solid lines refer to Lorentz fitting curves.

What is more, we have calculated the transient frequency-dependent complex photoconductivity parameters $\tilde{E}_{\mathrm{pump}}$ and $\tilde{E}_{\mathrm{without\ pump}}$ from the transmitted terahertz waveform under the conditions with and without the optical pumping, respectively. The complex Fourier transform of the time-dependent field is related to the complex conductivity $\tilde{\sigma}(\omega) = \sigma_{\mathrm{r}}(\omega) + \mathrm{i}\sigma_i(\omega)$, and given as follows:[24–27]

$$\frac{\tilde{E}_{\mathrm{pump}}(\omega)}{\tilde{E}_{\mathrm{without\ pump}}(\omega)} = \frac{n+1}{n+1+Z_0 \mathrm{d}\tilde{\sigma}(\omega)}, \tag{5}$$

where d is the thickness of the photo-excited layer (10 μm estimated based on the penetration depth of the 808-nm pump in Si),[28] $Z_0 = 377\ \Omega$ is the impedance of free space, and $n = 3.42$ is the refractive index of Si.[29–31] The conductivity is mainly determined by the real part ($\sigma_{\mathrm{r}}(\omega)$). Therefore, we plot the real parts of conductivity of the five samples. As illustrated in Fig. 6, in a range from 0.5 THz to 1.5 THz, we can see that the photo-excited conductivity is 3 orders of magnitude greater than the non-photo-excited one and decreases with increasing frequency, which is opposite to the result in Fig. 5. The blank silicon has the greatest conductivity, followed by the four BSs'. In addition, the four BS samples with different geometric structures show different electric properties from each other. The conductivity increases with increasing the size of surface geometry.

The Drude model is ordinarily suitable for two-dimensional free electron gas with complete momentum randomization following elastic scattering events. However, in the 10-μm photo-excited layer and micro/nano-conical surface structures in BS samples, more photo-excited electrons reflect from interfaces and surfaces. Such a backward scattering event can be modeled by modifying the Drude model according to Smith by including the persistence of velocity parameter to describe the scattering event.[32,33] The Drude Smith model is given by

$$\tilde{\sigma}(\omega) = \frac{Ne^2\tau/m^*}{1-\mathrm{i}\omega\tau}\left[1+\frac{c_1}{1-\mathrm{i}\omega\tau}\right], \tag{6}$$

where the parameter c_1 is a measure of persistence of the initial velocity of carrier after the first scattering event, which can also be called backscattering rate. Backscattering rate c_1 can vary from 0 (isotropic scattering, as in the Drude model) to -1 (full carrier backscattering), its negative value implies a predominance of backscattering. Additionally, N is the electron density, e is the elementary charge, m^* is the electron effective mass, and τ is the characteristic scattering time. The effective mass of electron is $0.26m_0$ for silicon. Here we can obtain the real part of the conductivity by

$$\sigma_{\mathrm{r}}(\omega) = \frac{Ne^2\tau/m^*}{1+\omega^2\tau^2}\left[1+\frac{c_1(1-\omega^2\tau^2)}{1+\omega^2\tau^2}\right]. \tag{7}$$

Fitting made with using equation (7) shows an extremely good matching of our data to the model, as shown in Fig. 6.

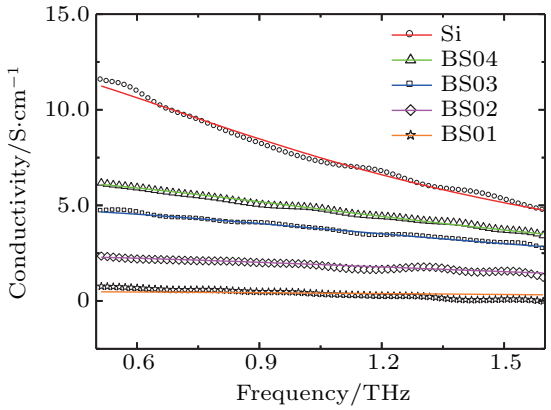


Fig. 6. (color online) Photo-excited conductivities of Si, BS01, BS02, BS03, and BS04 with optical pump, where solid lines represent Drude–Smith fitting curves.

Based on the curve fitting of photoconductivity $\sigma_{\mathrm{r}}(\omega)$ to the Drude–Smith model, fitting parameters of electron density N, characteristic scattering time τ, and back-scattering rate c_1 are derived and summarized in Table 1. The parameters N, τ, c_1,vary monotonically with conductivity. In order to illustrate the relationship between the carrier dynamics and the surface micro-structure geometry, we plot these fitting parameters against surface structure of sample in Fig. 7.

Table 1. Parameters for Drude–Smith fits of conductivity.

Sample	$N/(10^{16}/\mathrm{cm}^3)$	τ/fs	c_1
BS01	0.60	92.9	–0.17805
BS02	2.70	99.4	–0.16403
BS03	5.26	100.2	–0.12202
BS04	6.45	107.3	–0.11398
Si	9.18	141.8	–0.05404

Note: N is electron density; τ is scattering time; c_1 is backscattering rate.

According to Fig. 2, the absorption of BS at 808-nm wavelength is more than blank silicon's, but in a longer time window, the electron density is smaller in BS. Besides, with increasing the size of surface structure, the electron density N rises. As a result, one would assume that the recombination rates between electrons and holes in BS with different surface micro-structure sizes should be different from each other. The characteristic scattering time τ obtained from Drude–Smith fits turns longer with increasing the size of the surface structure. Nonetheless the variation of τ between BS remains small and the characteristic scattering time of the BS is much shorter than that of the blank silicon. It implies that the size of surface structure may be a key factor for an average time interval between collision events. At a flat surface without complex geometry or space confinement, for instance, the surface of blank silicon, the photo-generated carriers more easily move around hence scattering time becomes longer. As an additional contribution to the standard Drude term, c_1 describes the persistence of the initial velocity of carrier after of the first scattering event. The persistence of velocity is all negative (see the 4th column in Table 1). We attribute the negative values to preferential backscattering of the electrons after the collisions. A fraction, but not all, of the backward scattering is a result of the electron reflecting from the surfaces, grain boundaries or defects. It could also result from a Coulombic restoring force originating from positively charged holes or defects. This restoring force or backward scattering can be modeled by modifying the Drude model, according to Smith, by including a persistence of velocity parameter to describe the scattering event.[32] Here negative values of c_1 are plotted in Fig. 7(c), and the curve drops with increasing the size of surface structure, suggesting that the number of backscattering electrons diminish. In other words, less collisions occur at a surface with bigger surface microstructure than at a smaller sized counterpart. In contrast, the more the collisions, the lower the kinetic energy of optical-generated carriers is and the higher the recombination rate between electrons and holes. This correlates with longer scattering time interval, and consequently, there may be less carriers in BS surface with smaller micro-structures. The interpretation is fully consistent with the evolutions of N and τ, and $-c_1$.

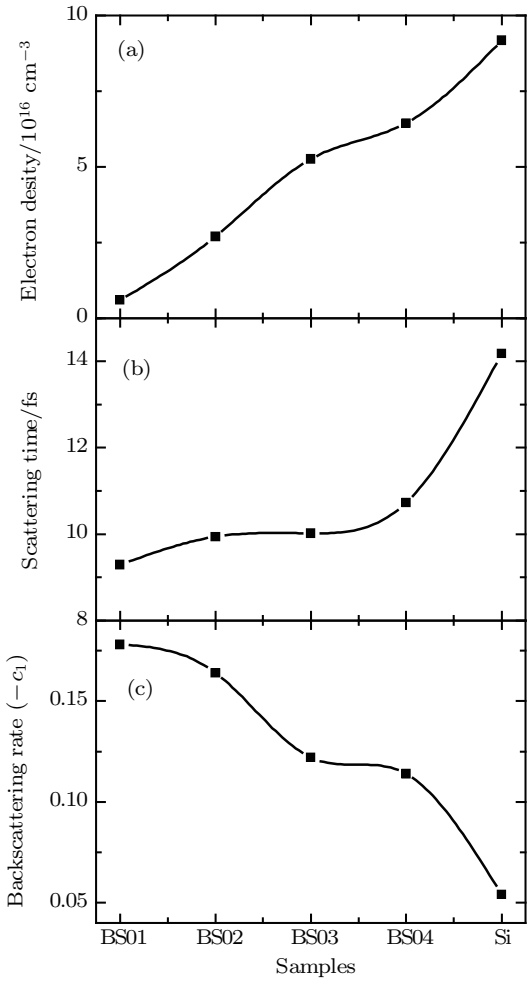


Fig. 7. Trends of electron density (N), scattering time (τ), backscattering rate ($-c_1$) of samples according to Table 1.

4. Conclusions

The optically induced changes in THz transmission and absorption of silicon wafers with two types of surfaces, i.e., unstructured blank silicon and micro-structured BS, are investigated at room temperature by using an NIR pump-terahertz probe system with an 808-nm CW laser pump. It is shown that BS structure causes not only a strong anti-reflection effect but also significant absorption enhancement at 808-nm wavelength due to localization effect and light trapping. The increases of the surface area and the photo-generated carrier concentration contribute to the absorption enhancement. Remarkably, with the optical pumping, the THz transmission spectra of blank silicon and BS are very different in the whole range of 0.5 THz–2.5 THz. It is proposed based on our measurements along with the model fitting that the carriers excited in BS surface with conical structure should have a stronger localization effect according to the backscattering behaviors in small-size micro-structures and the higher recombination rate due to increased electron interactions with other electrons, the interfaces and grain boundaries. Therefore, in the bigger conical geometry structure the excited carriers may move around more easily and as a consequence less collision would occur, which is related to higher THz absorption. Our work paves the way for a better understanding of the influence of the different geometrical- and optical-induced absorption of THz wave and the future applications of the black silicon.

References

[1] Li B J, Zhou M, Zhang W, Amoako G and Gao C Y 2012 *Appl. Surface Sci.* **263** 45
[2] Vorobyev A Y and Guo C L 2013 *Laser & Photon. Rev.* **7** 385
[3] Ma Y C, Si J H, Sun X H, Chen T and Hou X 2014 *Appl. Surf. Sci.* **313** 905
[4] Brongersma M L, Cui Y and Fan S H 2014 *Nat. Mater.* **13** 451
[5] Savin H, Repo P, von Gastrow G, Ortega P, Calle E, Garin M and Alcubilla R 2015 *Nat. Nanotechnol.* **10** 624
[6] Chen W H and Hong F C N 2016 *Solar Energy Materials & Solar Cells* **157** 48
[7] Blumroder U, Zilk M, Hempel H, Hoyer P, Pertsch T, Eichberger R, Unold T and Nolte S 2017 *Opt. Express.* **25** 6604
[8] Yang Y P, Zhang Z W, Shi Y L, Feng S and Wang W Z 2010 *Chin. Phys. B* **19** 043302
[9] Yang Y P, Wang W Z, Zhang Z W, Zhang L L and Zhang C L 2011 *J. Phys. Chem. C.* **115** 10333
[10] Trukhin V N, Bouravleuv A D, Mustafin I A, Kakko J P, Huhtio T, Cirlin G E and Lipsanen H 2015 *Appl. Phys. Lett.* **106** 1
[11] Gladun A D, Leiman V G and Arsenin A V 2008 *Physics*
[12] Baxter J B and Schmuttenmaer C A 2006 *Phys. Chem. B* **110** 25229
[13] Guo H C, Zhang X H, Liu W, Yong A M and Tang S H 2009 *J. Appl. Phys.* **106** 63
[14] Porte H P, Turchinovich D, Persheyev S, Fan Y C, Rose M J and Jepsen P U 2013 *IEEE Trans. Terahertz Sci. Technol.* **3** 331
[15] Kuzel P and Nemec H 2014 *J. Phys. D: Appl. Phys.* **47** 374005
[16] Lee W J, Ma J W, Bae J M, Jeong K S, Cho M H, Kang C and Wi J S 2013 *Sci. Rep.* **3** 1984
[17] Liu Y, Liu S, Wang Y, Feng G, Zhu J and Zhao L 2008 *Laser Phys.* **18** 1148
[18] Winkler M T, Sher M J, Lin Y T, Smith M J, Zhang H F, Gradecak S and Mazur E 2012 *J. Appl. Phys.* **111** 093511
[19] Yang Y P, Cui B, Geng Z X and Feng S 2015 *Appl. Phys. Lett.* **106** 111106
[20] Yang Y P, Lei X Y, Yue A and Zhang Z W 2013 *Sci. China-Phys. Mech. & Astron.* **56** 713
[21] Dorney T D, Bataniuk G, Mittleman M 2001 *J. Opt. Soc. Am. A* **18** 1562
[22] Yang Y P, Feng S, Feng h, Pan X C, Wang Y Q, Wang W Z 2011 *Acta Phys. Sin.* **60** 027802 (in Chinese)
[23] Balkanski M 1972 *Optical Properties of Solids* (New York) Chap. 8
[24] Zhou Q L, Shi Y L, Li T, Jin B, Zhao D M and Zhang C L 2009 *Sci. China-Phys. Mech. & Astron.* **52** 1944
[25] Walther M, Cooke D G, Sherstan C, Hajar M, Freeman M R and Hegmann F A 2007 *Phys. Rev. B* **76** 125408
[26] Cooke D G, Hegmann F A, Young E C and Tiedje T 2006 *Appl. Phys. Lett.* **89** 122103
[27] Ostroverkhova O, Cooke D G, Shcherbyna S, Egerton R F and Hegmann F A 2005 *Phys. Rev. B* **71** 035204
[28] Aspnes D E and Studna A A 1983 *Phys. Rev. B* **27** 985
[29] Grischkowsky D, Keiding S, M. Exter M and Fattinger C 1990 *Opt. Soc. Am. B* **7** 2006
[30] Ulbricht R, Hendry E, Shan J, Heinz T F and Bonn M 2017 *Rev. Mod. Phys* **89** 029901
[31] Joyce H J, Docherty C J, Gao Q, Hoe T H, Chennupati J, James L H, Herz L M and Johnston M B 2013 *Nanotechnology* **24** 1
[32] N V Smith 2001 *Phys. Rev. B* **64** 155106
[33] Zou X Q, Luo J S, Lee D W, Cheng C W, Springer D, Naritha S K, Cheong S A, Fan H J and Chia E E M 2012 *J. Phys. D: Appl. Phys.* 45